Cortisol Trajectories Measured Prospectively across Thirty Years of Female Development following Exposure to Childhood Sexual Abuse: Moderation by Epigenetic Age Acceleration at Midlife

Chad E. Shenk, Ph.D.;[1,2] John M. Felt, Ph.D.;[1] Nilam Ram, Ph.D.;[3,4] Kieran J. O'Donnell,[5,6] Ph.D.; Martin J. Sliwinski, Ph.D.;[1] Irina Pokhvisneva, M.Sc.;[7] Lizbeth Benson, M.S.;[1] Michael J. Meaney, Ph.D.;[7,8,9] Frank W. Putnam, M.D.;[10] & Jennie G. Noll, Ph.D.[1]

[1] = Department of Human Development and Family Studies, The Pennsylvania State University; [2] = Department of Pediatrics, The Pennsylvania State University College of Medicine; [3] = Department of Communications, Stanford University; [4] = Department of Psychology, Stanford University; [5] = Child Study Center, Yale University; [6] = Department of Obstetrics, Gynecology and Reproductive Sciences, Yale University; [7] = The Douglas Hospital Research Centre, Department of Psychiatry, McGill University; [8] = Child and Brain Developmental Program, Canadian Institute for Advanced Research; [9] = Singapore Institute of Clinical Sciences, Singapore; [10] = Department of Psychiatry, University of North Carolina School of Medicine

Declaration of Competing Interest: The authors declare that they have no conflict of interest.

Funding: Research reported in this manuscript was supported by the National Institutes of Health under Award Numbers R01AG059682 (Shenk), R01HD072468 (Noll); R01AG04879 (Noll), and P50HD089922 (Noll). The content is solely the responsibility of the authors and does not necessarily represent the official views of the National Institutes of Health.

Corresponding Author:

Chad Shenk, Ph.D.
The Pennsylvania State University
115 Health and Human Development Building
University Park, PA 16802
Email: ces140@psu.edu
Phone: +1 814 865 9688
Fax: +1 814 865 2530

Highlights

- Resting state cortisol concentrations were obtained prospectively over 30 years
- Childhood sexual abuse and epigenetic age acceleration were involved in cortisol function
- Novel dimensions of deviations in normative cortisol growth are reported
- Key assumptions of the biological embedding of early life adversity were supported

Abstract

Lasting changes in the hypothalamic-pituitary-adrenal (HPA) axis are a potential indication of the biological embedding of early life adversity, yet, prospective and repeatedly collected data are needed to confirm this relation. Likewise, integrating information from multiple biological systems, such as the HPA axis and the epigenome, has the potential to identify individuals with enhanced embedding of early life adversity. The current study reports results from the Female Growth and Development Study, a 30-year prospective cohort study of childhood sexual abuse (CSA). Females exposed to substantiated CSA and a demographically-similar comparison condition were enrolled and resting state cortisol concentrations were sampled on seven subsequent occasions across childhood, adolescence, and adulthood. Differences in participants' cortisol trajectories were examined in relation to prior CSA exposure and DNA methylation-derived epigenetic age acceleration at midlife. Bilinear spline growth models revealed a trajectory where cortisol secretion increased until approximately age twenty and then declined into mid-life, consistent with normative trends. However, cortisol concentrations peaked at a lower level and transitioned to the decline phase at an earlier age for females in the CSA condition with increased epigenetic age acceleration. Robustness tests across three independent measures of epigenetic age acceleration demonstrated similar results for lower peak cortisol levels and earlier ages at transition. Results suggest that CSA is associated with significant changes in HPA-axis activity over extended periods of time with these changes most pronounced in females with accelerated epigenetic aging in mid-life. Implications for biological embedding models of early life adversity and adulthood health are discussed.

Keywords: Childhood sexual abuse, cortisol, epigenetic age acceleration

1. Introduction

Child maltreatment is a severe form of early life adversity affecting 650,000 children in the U.S. annually (U.S. Department of Health and Human Services, 2021). The risks associated with child maltreatment are well-established, including adverse physical and behavioral health in childhood (Alisic et al., 2014; Oh et al., 2018) as well as sustained risks for many of the major causes of morbidity and mortality in adulthood (Gilbert et al., 2009; Hughes et al., 2017). Models on the biological embedding of early life adversity (Del Giudice et al., 2011; McEwen, 2007) suggest that the immediate and sustained risks that follow child maltreatment are the result of multi-factorial changes in major biological systems that respond to environmental challenge and are associated with long-term health. In particular, the hypothalamic-pituitary-adrenal (HPA) axis, and specifically its end product cortisol, has long been examined as a neuroendocrine pathway sensitive to child maltreatment (Bernard et al., 2017; Miller et al., 2007) and associated with both physical (Adam et al., 2017; Dahmen et al., 2018) and behavioral health (Lippard & Nemeroff, 2020; Pan et al., 2018). However, research supporting associations between child maltreatment and changes in cortisol secretion is largely based on cross-sectional or short-term longitudinal studies that cannot examine a key assumption of biological embedding models, namely, if and how long-term changes in cortisol secretion follow exposure to child maltreatment.

Resting state cortisol secretion follows a normative, non-linear trajectory characterized by increasing output between approximately ages five to twenty years before peaking and then declining between ages twenty to forty-five (Miller et al., 2016). To our knowledge, there has not been a prospective, longitudinal study that has examined whether prior exposure to child maltreatment alters this normative pattern of cortisol secretion during this same age range. One study by Trickett and colleagues (2010) used data from the Female Growth and Development Study (FGDS; Trickett et al., 2011), a thirty-year prospective cohort study of females exposed to childhood sexual abuse (CSA), that repeatedly sampled resting state cortisol concentrations between ages six to thirty. Relative to females in a non-CSA comparison condition, this study identified a cortisol hypersecretion profile in the years immediately following exposure to CSA. However, individuals with this initial hypersecretion profile transitioned to a

hyposecretion profile by age thirty, at which time significant differences in cortisol trajectories were observed across conditions. These results provide valuable support to models of the biological embedding of early life adversity by showing that CSA is systematically related to long-term changes in the normative trajectory of resting state cortisol secretion. While many factors are likely involved, these results also offer a plausible explanation for inconsistent findings on hyper- vs. hypocortisol secretion profiles reported in cross-sectional and short-term longitudinal research (Holochwost et al., 2020; O'Donnell et al., 2013), showing that both profiles can be observed when an extended period of assessment with the same individuals is utilized. Thus, prospective research examining cortisol secretion over extended periods of time can provide a strong test of the long-term adaptation of the HPA axis following exposure to child maltreatment, and specific dimensions of that adaptation, posited by models on the biological embedding of early life adversity.

However, variation exists in the extent to which individuals demonstrate lasting change in cortisol secretion subsequent to child maltreatment (Kuzminskaite et al., 2020), suggesting that examination of additional biological systems may help distinguish those experiencing the greatest long-term adaptation of HPA axis function from those who do not. Epigenetic age acceleration, that is, biological aging not attributable to chronological aging, serves as a potential candidate system that can explain such variation in HPA axis function following exposure to child maltreatment. Epigenetic age acceleration is derived from variation in DNA methylation across many different cytosine-phosphate-guanine (CpG) dinucleotide sites across the genome. Given the range and location of CpG sites included, estimates of epigenetic age acceleration therefore serve as an integrative biomarker of multiple biological processes, including the activity of specific metabolic signaling pathways, the proportion of stem cells within a given tissue or biosample, and systemic inflammation (Lu et al., 2018; Raj & Horvath, 2020; Zannas, 2019), that can indirectly influence HPA-axis activity (Silverman et al., 2005; Ulrich-Lai & Ryan, 2014). Furthermore, increased cortisol secretion has been associated with accelerations in epigenetic aging (Davis et al., 2017), potentially through enhanced variation of DNA methylation at CpG sites located within or near glucocorticoid response elements included in estimates of epigenetic age acceleration

(Zannas et al., 2015). This evidence suggests that measures of epigenetic age acceleration may be particularly sensitive to long-term adaptations of HPA axis activity and therefore capable of identifying individuals showing the greatest change from normative trends in cortisol secretion following exposure to child maltreatment. An additional advantage of using epigenetic age acceleration to identify individuals with the greatest change in cortisol secretion following exposure to child maltreatment is the ability of this biomarker to predict different domains of subsequent adult health. First generation epigenetic aging estimators (Hannum et al., 2013; Horvath, 2013) were trained to predict chronological age yet serve as a better predictor of adult mortality than chronological age (Chen et al., 2016; Marioni et al., 2015). Second generation epigenetic aging estimators (Levine et al., 2018; Lu et al., 2019) on the other hand have been developed to integrate both age-related changes in DNA methylation as well as DNA methylation-based biomarkers of common domains of adult morbidity and mortality. These estimators therefore have the potential to serve an important translational bridge, that is, connecting individuals with the greatest long-term adaptation of HPA axis activity following child maltreatment with reliable biomarkers of adult morbidity and mortality. Such knowledge could inform the targeted prevention of adverse adult health associated child maltreatment, particularly for those who display accelerations in epigenetic aging.

The current study combined newly available data on cortisol secretion and epigenetic aging biomarkers obtained in the most recent wave of FGDS data collection with the existing longitudinal data to advance research on the biological embedding of early life adversity in two important ways. One, based on prior research (Miller et al., 2016), the current study characterized the normative, non-linear trajectory of resting state cortisol secretion, and the inter-individual differences therein, from childhood to mid-life for females. This provides a unique opportunity to examine prospectively the changes in cortisol secretion during this time and following exposure to CSA. Two, the current study examined whether epigenetic age acceleration at mid-life could identify inter-individual and group-differences exhibiting the greatest deviation from the expected non-linear cortisol trajectories associated with the biological embedding of CSA. The current study first tested models using the Horvath epigenetic aging clock (Horvath, 2013) given the inclusion of multiple glucocorticoid-sensitive CpGs in this estimator and then checked the

robustness of these results by testing models across multiple, distinct epigenetic age estimators: Hannum (Hannum et al., 2013), PhenoAge (Levine et al., 2018), and GrimAge (Lu et al., 2019). The primary aim of this study was to test the relation between CSA status and subsequent changes in cortisol secretion over 30 years of female development and whether accelerations in epigenetic aging at mid-life could identify those individuals most sensitive to CSA-related HPA-axis change.

2. Material and Methods

2.1. Study Design, Recruitment, and Sample

The FGDS began data collection in 1987 using an accelerated cross-sequential prospective cohort design (McArdle & Woodcock, 1997) wherein an age-heterogenous sample of females were followed longitudinally as they moved through multiple stages of development. Females exposed to substantiated CSA (n = 82) were referred by Child Protective Services (CPS) agencies in the greater Washington, D.C. area. Comparison females (n = 84) were recruited via advertisements in community newspapers and posters placed in welfare, daycare, and community facilities in the same neighborhoods in which the females exposed to CSA resided. Eligibility criteria included: (1) age 6-16 years; (2) referral and study participation within six months of disclosing CSA; (3) substantiated CSA involving genital contact and/or penetration, (4) perpetration by a family member, defined as a parent, grandparent, older sibling, live-in boyfriend, or uncle; (5) study participation by a non-abusing caregiver, and (6) no evidence of sexual abuse or prior contact with CPS for females in the comparison condition.

There have been seven data collection assessments with the FGDS cohort throughout childhood, adolescence, and adulthood (T1-T7; 1987-2019). Following completion of the T3 data collection assessment, it was discovered that four females in the CSA condition did not meet initial eligibility criteria (three experienced non-familial sexual abuse, one exceeded the age range) and three females in the comparison condition self-reported a history of exposure to CSA. In response, twenty-one new comparison females were enrolled at the T4 assessment and followed longitudinally to fortify the sample. An additional eight females in the comparison condition self-reported exposure to CSA during T4-T7. To maintain fidelity with the initial eligibility criteria, and to avoid potential bias from contamination (Shenk

et al., 2016), these fifteen females (n = 4 in CSA, n = 11 comparison) were removed from statistical modeling in the current study, resulting in a total available sample size of N = 172 (CSA condition: n = 82 – 4 = 78; Comparison condition: n = 84 – 3 + 21 – 8 = 94). The racial and ethnic demography for this total sample is 54.1% White, 42.4% Black, 2.9% Hispanic, and 0.6% Asian. There were no statistically significant differences across CSA and comparison conditions on age at enrollment (including at T1 and at T4), Hollingshead socioeconomic status scores at enrollment (including at T1 and at T4), or racial minority status (all p's > .138).

A total of n = 132 females completed the T7 assessment (M_{age} = 36.82, SD = 3.64), when blood samples for assaying genetic and epigenetic data were collected (see below). There were no significant differences on age at enrollment (including at T1 and at T4), socioeconomic status at enrollment (including at T1 and at T4), racial minority status, or CSA status between those participants who completed the T7 assessment and those who did not (p's > .254). Of the females completing T7, n = 86 provided viable blood samples for describing genetic and epigenetic variation, consented to long-term storage of samples for use in the present analyses, and were not among those fifteen participants removed from statistical modeling. Thus, all subsequent models are based on n = 86. There were no significant differences on age, racial minority status, or CSA status (socioeconomic status was not measured at T7) between those who completed the T7 assessment and were included in the present statistical models and those that were not (p's >. 349).

2.2. Measurement of Cortisol

Cortisol concentrations were originally sampled using serum obtained from whole blood at FGDS T1-T3 (1987-1992). This sampling method switched to salivary assessments for FGDS T4-T7 (1996-2019) given the development of this technology to obtain cortisol concentrations non-invasively yet produce strong correlations with concentrations obtained from blood-based measures (Bober et al., 1988; Goodyer et al., 1996). However, sampling cortisol via whole blood and saliva required the use of a conversion formula so that obtained cortisol data across T1-T7 can be used in the same statistical modeling framework. Data and equations provided in Salimetrics® U.S. Food and Drug Administration

approved salivary cortisol enzyme immunoassay investigative device (FDA 510[k] #K031348) provided a formula for converting salivary cortisol concentrations to unbound serum cortisol concentrations (Trickett et al., 2010):

$$(\text{serum } \mu g/dL) = 5.177 + 15.132*(\text{saliva } \mu g/dL), \quad (1)$$

2.2.1. Serum cortisol (T1–T3)

Following arrival to the study visit and consenting procedures, all females completed a 30-minute resting period before providing samples of unbound serum cortisol via an indwelling catheter inserted into a forearm vein. The majority of samples were obtained in the morning hours between 9:00 a.m. and 12:00 p.m. Once collected, samples were refrigerated until centrifugation, which occurred within 2 hours, and then frozen at -70°C until assayed by radioimmunoassay by Hazleton Laboratories (Vienna, VA). The average intra- and inter-assay coefficients of variation were 3.4% and 12.3%, respectively.

2.2.2. Salivary cortisol (T4–T6)

Following arrival for the study visit and consenting procedures, all females completed a 30-minute resting period prior to providing stimulant-free saliva via passive drool. Consistent with T1-T3, the majority of samples were collected in the morning between 9:00 a.m. and 12:00 p.m. All samples were stored at -70°C until assayed in duplicate by enzyme immunoassay by Salimetrics® (State College, PA). The assay used 25 mL of saliva per determination and had average intra- and inter-assay coefficients of variation of 5.10% and 8.20%, respectively. Thirteen (1.7%) cortisol samples obtained from T4-T6 were above 26 μg/dL, designated as statistical outliers, and removed from statistical analyses.

2.2.3. Salivary cortisol (T7)

Stimulant-free saliva was sampled via salivette as part of a two-day, five sample, in-home protocol assessing diurnal cortisol rhythms where three samples were obtained in the morning, one in the afternoon, and one in the evening prior to bedtime. Samples were shipped to research staff and stored at -70°C until assayed in duplicate using enzyme immunoassay (Salimetrics®). The intra- and inter-assay coefficients of variation for the T7 samples ranged from 1.7%-5.0% and 2.8%-8.9%, respectively. To

align the data collection protocol as closely as possible to the resting-state sampling procedures of T1-T6, T7 samples provided approximately one hour after awakening (the third of five samples) were averaged over the two consecutive days and included in statistical modeling. If there was only one day of cortisol sampled one hour after awakening, that single estimate was used in statistical modeling.

2.3. Genomic Analyses

Whole blood samples were collected via venipuncture at the T7 assessment and then placed in dry ice shipment containers for transport to long-term freezer storage and ultimate extraction. Genomic DNA was extracted from whole blood using a semi-automated approach (Qiasymphony, Qiagen) and purity assessed using a nanophotometer (ImplenP300, Implen).

2.3.1. Genotyping

The Infinium Global Screening Array v1.0 (Illumina, San Diego CA, USA) was used to characterize variation at 690,364 markers across the genome according to manufacturer's guidelines. Individuals with low genotyping rates (<95%) and single nucleotide polymorphisms (SNPs) showing significant deviation from Hardy-Weinberg equilibrium (HWE, p-value < 1×10^{-30}) were excluded. Similarly, SNPs with high rates of missing data (>5%) were excluded. Quality control of genetic data was performed using PLINK 1.9 (Chang et al., 2015). Imputation of additional variants was performed using the Sanger Imputation Service with Haplotype Reference Consortium (release 1.1; http://www.haplotype-reference-consortium.org/participating-cohorts) panel (McCarthy et al., 2016). SNPs with imputation accuracy score of less than 0.8 were excluded. Imputed genotype probabilities were converted to hard-called genotypes using posterior genotype probability above 0.90. Population structure was described using principal component analysis (Patterson et al., 2006) of a pruned set of genotyped SNPs with a minor allele frequency > 5% in low linkage disequilibrium (r^2<0.20) with a 50 kilobase sliding window and an increment of 5 SNPs. Population structure was best described by the first three principal component scores (PC1, PC2, PC3), which were included as covariates in specified analyses.

2.3.2. DNA Methylation

The Infinium Methylation EPIC Beadchip (EPIC array, Illumina, San Diego CA, USA) was used to describe variation in DNA methylation across the genome. Genomic DNA (1ug) from whole blood was treated with sodium bisulfite using the Zymo EZ-96 DNA Methylation Kit™ (Zymo Research, Orange, CA, USA) with 200ng of bisulfite-treated DNA amplified, fragmented, and hybridized on the EPIC array. Raw intensity values (idat files) were directly loaded into R for quality control and normalization using the Minfi package (Bioconductor). Standard Minfi quality control (QC threshold < 10.5) was conducted and poorly performing samples were removed. All samples had a call rate >99%. Poorly performing probes were identified as those which had a call rate <75%. Biological sex was predicted using DNA methylation of the sex chromosomes and matched the reported sex in all samples. Likewise, a selection of SNPs shared between the 850K array and genotyping array showed 100% within-person concordance. Background correction and dye-bias adjustment was carried out using Noob (Triche et al., 2013).

2.3.3. Epigenetic Age Acceleration

Four measures of epigenetic age acceleration were generated using a publicly available tool (https://dnamage.genetics.ucla.edu/home): 1) Horvath, 2) Hannum, 3) PhenoAge, and 4) GrimAge clocks. The current analysis focuses on measures of age acceleration, that is, residualized scores of biological aging determined by DNA methylation after accounting for each person's chronological age at the time of biological sample collection. These four epigenetic age estimates are correlated (r = .17-.45; Lu et al., 2019) but are derived from DNA methylation at largely non-overlapping sites across the genome. Each measure of epigenetic age acceleration was grand-mean centered. For each measure, positive values of epigenetic age acceleration indicate faster aging (acceleration) and negative values indicate slower aging (deceleration). Cell-type heterogeneity across samples were deconvolved using a well-established reference-based approach (Houseman et al., 2012) with proportions of cell-types included where appropriate. All estimates of epigenetic age acceleration included as main and interaction terms in subsequent modeling were tested as continuous measures but are graphically represented as model-implied predictions at ±1SD scores in subsequent Figures.

2.4. Data Analysis

Chronological age at each FGDS assessment was calculated as the difference between the date of data collection and an individual's date of birth and centered at age 16 years (the center of the data) in all analyses. Across the repeated measures, chronological age ranged from 6 to 45 years. Group and individual differences in the developmental trajectories of resting state cortisol were examined using a bilinear spline growth model (Grimm et al., 2017). In this model, age-related changes in cortisol concentrations were modeled using a non-linear function that describes each individual's trajectory as consisting of two distinct phases of linear change, an early phase where cortisol increases and a later phase where cortisol decreases. This modeling approach therefore provides a valuable framework for estimating the expected age-related changes in resting state cortisol secretion for females ages 6-45 years (Miller et al., 2016), particularly when considering the additional, repeated assessments of resting state cortisol concentrations over time (Riis et al., 2020). The bilinear spline model also provides an opportunity to model individual deviations from the expected trajectory of resting state cortisol secretion. Specifically, individual trajectories may differ in four ways: (1) the rate of increase in cortisol during the earlier, pre-knot phase, (2) the level of cortisol at the knot point, (3) the age at the knot point, and (4) the rate of decrease during the latter, post-knot phase, providing multiple dimensions for how the biological embedding of CSA might be observed in the HPA-axis. Analytically, the up to seven repeated measures of cortisol for individual *i* at occasion *t* were modeled as:

$$\mathrm{Cortisol}_{it} = \beta_{0i} + \beta_{1i}(\mathrm{ChronAge}_{it} - \beta_{3i}) + \beta_{2i}\sqrt{(\mathrm{ChronAge}_{it} - \beta_{3i})^2} + e_{it} \quad (2)$$

where β_{0i} is a person-specific intercept that indicates the expected value of cortisol for person *i* at the knot point; β_{1i} is a person-specific slope that describes the rate of change in cortisol (per year) during the pre-knot phase; β_{2i} is a person-specific slope that describes the difference in the rate of change between the pre- and post-knot phases; β_{3i} is a person-specific timing parameter that indicates the age at which an individual transitions from the pre-knot phase to the post-knot phase; and e_{it} are occasion-specific

residuals. In turn, the person-specific intercepts, pre-knot slopes, post-knot slopes, and knot-point timing were modeled as:

$$\begin{aligned}
\beta_{0i} &= \gamma_{00} + \gamma_{01}(\text{Group}_i) + \gamma_{02}(\text{EpigAge}_i) + \gamma_{03}(\text{Group}_i * \text{EpiAge}_i) + \gamma_{04}(\text{PC1}_i) \\
&\quad + \gamma_{05}(\text{PC2}_i) + \gamma_{06}(\text{PC3}_i) + u_{0i} \\
\beta_{1i} &= \gamma_{10} + \gamma_{11}(\text{Group}_i) + \gamma_{12}(\text{EpigAge}_i) + \gamma_{13}(\text{Group}_i * \text{EpiAge}_i) + u_{1i} \\
\beta_{2i} &= \gamma_{20} + \gamma_{21}(\text{Group}_i) + \gamma_{22}(\text{EpigAge}_i) + \gamma_{23}(\text{Group}_i * \text{EpiAge}_i) + u_{2i} \\
\beta_{3i} &= \gamma_{30} + \gamma_{31}(\text{Group}_i) + \gamma_{32}(\text{EpigAge}_i) + \gamma_{33}(\text{Group}_i * \text{EpiAge}_i) + u_{3i}
\end{aligned} \tag{3}$$

where γ_{00}, γ_{10}, γ_{20}, γ_{30} indicate the prototypical intercept, pre-knot slope, post-knot slope, and knot-point timing (conditional on predictors); $\gamma_{01,}$ $\gamma_{11,}$ $\gamma_{21,}$ and $\gamma_{31,}$ indicate differences in the intercept, pre-knot slope, post-knot slope, and knot-location, respectively, between CSA and comparison conditions (*Group*); $\gamma_{02,}$ $\gamma_{12,}$ $\gamma_{22,}$ and γ_{32} indicate how the intercepts, pre-knot slopes, post-knot slopes, and knot locations (level, timing) are related to differences in epigenetic age acceleration (*EpiAge*); $\gamma_{03,}$ $\gamma_{13,}$ $\gamma_{23.}$ and γ_{33} indicate if and how those relations differ across CSA conditions; and γ_{04}, $\gamma_{05,}$ and γ_{06} indicate how population structure is associated with cortisol levels. Residual terms u_{0i}, u_{1i}, u_{2i}, and u_{3i} capture other unexplained individual differences that are assumed multivariate normally distributed.

Model parameters were estimated in the Bayesian framework using the *brms* package in R (Bürkner, 2017). Four chains, each with 50,000 iterations (first 25,000 used as burn-in) and a thinning interval of 1, provided posterior distributions with 25,000 samples for inference. Priors included a half Student's-*t* prior with three degrees of freedom and scale parameter of 10 for the standard deviations of the random effects, a Lewandowski-Kurowieka-Joe prior with parameter of 1 for the correlations among random effects, a normal prior with a location of 10 and scale of 5 for the intercept to ensure the parameter space was positive, and normal priors with a location of 0 and scale of 5 for all other parameters. Incomplete data were treated using standard missing at random assumptions. Convergence of Monte Carlo Markov Chain (MCMC) algorithms were determined through graphical examination of the MCMC chains and assurance that all rhat values were below 1.10 (Bürkner, 2017). Following the

Bayesian framework, results and inferences are derived from description of the central tendency (mean) of the posterior distribution for each parameter (γ), standard errors of the mean (SE), and the 95% credibility intervals ($CI_{95\%}$). Inference about the fixed effects parameters makes use of the probability of direction (PD) for each parameter, an index reflecting the certainty that a parameter is above or below 0, with the lower bound (PD = .50) indicating no certainty and the upper bound (PD = 1.0) indicating complete certainty. Note that the statistical power to detect an effect in the Bayesian framework does not rely on large samples, as information from prior probability distributions are incorporated into the models (Kruschke, 2015). Frequentist notions of statistical power for each effect can be observed indirectly via the width of the credibility intervals and the PD. For example, when power is "high," there are smaller credibility intervals and the PD becomes directionally closer to either 0.5 or 1.0. When power is "low", credibility intervals are wider and the PD may fall anywhere along the range between 0.5 and 1.0. For the models presented in the current manuscript, the PD is emphasized as it provides a very specific quantification of statistical power and certainty with this specific sample.

3. Results

3.1. Age-related Change in Cortisol from Childhood to Mid-life

The prototypical developmental trajectory for cortisol was described by four parameters: an intercept (γ_{00} = 12.03, $CI_{95\%}$[11.31, 12.75], PD = 100%), positive linear pre-knot slope (γ_{10} = 0.26, $CI_{95\%}$[00.17, 0.35], PD = 100%), negative linear post-knot change in slope (γ_{20} = -0.36, $CI_{95\%}$[-0.46, -0.27], PD = 100%), and a knot-location (γ_{40} = 3.44, $CI_{95\%}$[1.85, 5.52], PD = 99.82%). As shown in Figure 1, the cortisol concentrations for the prototypical individual in the sample increased until age 19.44 (centering age of 16 + 3.44) where cortisol concentrations peaked at 12.03 μg/dL, and then began to decrease. Importantly, and as evident from the raw data trajectories shown in light gray in Figure 1, there were substantial individual differences in all four aspects of the cortisol change trajectories: random effects for the intercept (σ_{u0} = 0.75, $CI_{95\%}$[0.04, 1.81]), the pre-knot slope (σ_{u1} = 0.06, $CI_{95\%}$[0.00, 0.14]), the post-knot slope (σ_{u2} = 0.06, $CI_{95\%}$[0.00, 0.17]), the knot-location (σ_{u3} = 1.12, $CI_{95\%}$[0.04, 2.98]), and the residuals (σ_{e} = 3.39, $CI_{95\%}$[3.11, 3.68] .

3.2 Moderation by Epigenetic Age Acceleration

Results from the bilinear spline models with sexual abuse status (CSA vs. comparison) and epigenetic age acceleration (four separate clocks) as person-level predictors are shown in Tables 1 and 2 as well as Figures 2 and 3.

3.2.1. Horvath Clock

There was evidence (PD = 88.80%) that epigenetic age acceleration, as indicated by the Horvath clock, moderated the association between CSA status and the pre-knot linear slope. Among females in the CSA group, accelerations in epigenetic aging were associated with a steeper pre-knot linear slope (γ_{13} = 0.04, $CI_{95\%}$[-0.03, 0.12]). There was also evidence (PD = 86.66%) that epigenetic age acceleration moderated the association between CSA status and the age of transition (knot point) between the early and late phases of change. Among females in the CSA group, accelerations in epigenetic aging were associated with an earlier transition from the pre- to post-knot phase of change (γ_{33} = -0.77, $CI_{95\%}$[-2.06, 0.64]). There was also evidence (PD = 93.13%) that epigenetic age acceleration moderated the association between CSA status and the level of cortisol at the knot point. Among females in the CSA condition, accelerations in epigenetic aging were associated with lower levels of cortisol concentrations at the knot point (γ_{03} = -0.39, $CI_{95\%}$[-0.89, 0.15]).

3.2.2. Hannum Clock

There was very weak evidence (PD = 64.82%) that epigenetic age acceleration, as indicated by the Hannum clock, moderated the association between CSA status and the pre-knot linear slope (γ_{13} = 0.08, $CI_{95\%}$[-0.10, 0.36]) with no evidence that it moderated the post-knot linear slope (γ_{23} = -0.04, $CI_{95\%}$[-0.32, 0.16], PD = 53.46%). With the Hannum clock, there was evidence (PD = 92.68%) that epigenetic age acceleration moderated the association between CSA status and the level of cortisol at the knot point (γ_{03} = -0.49, $CI_{95\%}$[-1.15, 0.18]). There was not much evidence (PD = 66.22%) that epigenetic age acceleration moderated the association between CSA status and the timing of the transition from the pre- to the post-knot phase (γ_{33} = -0.65, $CI_{95\%}$[-3.11, 1.93]).

3.2.3. PhenoAge Clock

There was evidence (PD = 84.72%) that epigenetic age acceleration, as indicated by the PhenoAge clock, moderated the association between CSA status and the pre-knot linear slope. Among females in the CSA condition, accelerations in epigenetic aging were associated with a steeper pre-knot linear slope (γ_{13} = 0.02, $CI_{95\%}$[-0.02, 0.05]). There was also evidence (PD = 87.87%) that epigenetic age acceleration moderated the association between CSA status and the post-knot linear slope (γ_{23} = -0.02, $CI_{95\%}$[-0.06, 0.01]), and the association between CSA status and the timing of the knot point (γ_{33} = -0.37, $CI_{95\%}$[-0.96, 0.34], PD = 88.51%). However, there was not much evidence (PD = 69.01%) that epigenetic age acceleration moderated the association between CSA status and the level of cortisol at the knot point (γ_{03} = -0.07, $CI_{95\%}$[-0.36, 0.25]).

3.2.4. GrimAge Clock

There was not much evidence (PD = 67.99%) that epigenetic age acceleration, as indicated by the GrimAge clock, moderated the association between CSA status and the pre-knot linear slope (γ_{13} = 0.01, $CI_{95\%}$[-0.04, 0.07]), between CSA status and the post-knot linear slope (γ_{23} = -0.01, $CI_{95\%}$[-0.07, 0.04], PD = 67.89), or between CSA status and the level of cortisol at the knot point (γ_{03} = -0.09, $CI_{95\%}$[-0.45, 0.28], PD = 70.66). There was evidence (PD = 86.62) that epigenetic age acceleration moderated the association between CSA status and the timing of the knot point (γ_{33} = -0.40, $CI_{95\%}$[-1.18, 0.38]).

4. Discussion

The current study leveraged the prospective, longitudinal design of the FGDS, which followed females with and without substantiated cases of CSA from childhood to mid-life to test key assumptions within current models of the biological embedding of early life adversity (Del Giudice et al., 2011; McEwen, 2007). Specifically, this study described inter-individual differences in intra-individual change in resting state cortisol secretion over thirty years of female development following exposure to CSA. Furthermore, this study provided a robust assessment of whether examining additional biological systems, namely epigenetic age acceleration as characterized by four different clocks, could reliably identify those individuals who showed more pronounced CSA-associated changes in resting state cortisol secretion during this time. The strengths of this study include objective measurements of all key study variables,

such as the use of independent ratings of CSA status, determination of cortisol secretion and epigenetic age acceleration through innovative assays and arrays, as well as the prospective cohort design spanning several periods of human development. Based on these strengths and corresponding study results, there are several important directions for future research and implications for models of the biological embedding of early life adversity.

One, the current study extends the prospective examination of the biological embedding of early life adversity to include an age range of nearly forty years that spans childhood, adolescence, and adulthood, illustrating the long-term changes in HPA axis function across several periods of female development. Specifically, this study modeled the normative, non-linear, age-related changes in resting state cortisol secretion for females aged six to forty-five years (Miller et al., 2016) and then demonstrated the inter-individual and group-based deviations from this normative trend as an indication of the biological embedding of early life adversity in the HPA axis. Advancing the longitudinal modeling of HPA axis change following exposure to CSA, a bilinear spline growth model (Grimm et al., 2017) characterized the observed longitudinal cortisol trajectories with respect to: (1) an earlier phase during childhood and young adulthood where cortisol increased, (2) a later phase during young adulthood and mid-life where the rate of change in cortisol decreased, (3) the age at which the transition from the earlier to the later phase occurred, and (4) the level of cortisol concentrations at this transition point. This non-linear growth modeling approach, aided by the repeated assessment of cortisol concentrations from the same individuals over time (Riis et al., 2020), therefore provides important information on different dimensions of cortisol change across childhood, adolescence and adulthood. The results from this study therefore provide new knowledge about how exposure to early life adversity, namely CSA, may be embedded in the HPA axis long-term and how to characterize the specific dimensions of that embedding in a way that may ultimately relate to adverse adulthood health.

Two, the current study examined multiple biological systems following exposure to early life adversity to identify individuals who showed the most pronounced CSA-related changes from childhood to adulthood according to specific dimensions of resting state cortisol secretion. Prior exposure to CSA

was associated with lower peak levels of cortisol concentrations at the transition between the early and later phases of cortisol secretion and an earlier transition to the decline phase by three to four years for females with accelerated epigenetic ages. These findings suggest that epigenetic age acceleration may be an important mid-life biomarker that can be used to identify individuals who experienced the most pronounced biological embedding of CSA in the HPA-axis from childhood to adulthood (Anacker et al., 2014; Gassen et al., 2017). These results were generally observed across the four epigenetic age acceleration clocks examined in this study, providing evidence for the robustness of differences in the peak level and age at transition for cortisol secretion following CSA. However, the results for epigenetic age acceleration were more prominent for some clocks compared to others. For example, results on the peak level of cortisol at the transition point was more evident for the Horvath and Hannum clocks whereas the timing of the transition point was more evident for the Horvath, GrimAge, and PhenoAge clocks. These differences may be explained based on how each individual clock was constructed. The Horvath clock includes glucocorticoid sensitive CpGs (Horvath, 2013), which may explain why it was associated with both the peak level of cortisol concentrations at the transition point and the age at which the transition point occurred. Thus, this clock may be more sensitive to detecting long-term changes in cortisol function than other clocks that do not include or sample glucocorticoid sites to the same degree. Similarly, the PhenoAge and GrimAge clocks are informed by variation in DNA methylation associated with both chronological age as well as health and disease-related phenotypes (Levine et al., 2018; Lu et al., 2019). Thus, epigenetic age acceleration estimates that are sensitive to detecting changes in the timing of the transition from increasing to decreasing cortisol secretion and also trained to predict adulthood health may be most useful in assessing how the biological embedding of CSA in the HPA axis is related to key indicators of adulthood health.

The biological mechanisms explaining both the normative changes in resting state cortisol secretion, as well as deviations from this normative pattern, reported in this study remain largely unknown. However, there are implications from this study that offer important avenues for future research to uncover such mechanisms. Although not always observed (Rosmalen et al., 2005), there is evidence

that the onset of puberty may explain the normative increase in resting state cortisol secretion observed between childhood and late adolescence prior to declining in early adulthood (Schreiber et al., 2006; Törnhage, 2002). The increase in cortisol production during this time is likely the result of increased production of gonadal steroids, specifically estrogen, associated with pubertal onset, given the modulating function of estrogen on circulating cortisol concentrations and the overall coordination between feedback mechanisms in the hypothalamic-pituitary-gonadal and HPA axes (Handa & Weiser, 2014; Simmons et al., 2015; Young, 1995). Interestingly, females exposed to CSA in the FGDS cohort began puberty eight to twelve months earlier, on average, than females the non-CSA condition (Noll et al., 2017), offering a potential explanation for why cortisol secretion would subsequently transition to the decline phase earlier for females in the CSA condition. Results of this study also suggest that exposure to CSA disrupts the normative production of resting state cortisol. One possible explanation for this is that prolonged hypersecretion of cortisol immediately following CSA can lead to lasting changes in the HPA axis (Trickett et al., 2010), potentially through enhanced negative feedback sensitivity (Fries et al., 2005), that ultimately produce an attenuation of cortisol output (Kaess et al., 2018). This explanation is consistent with the results reported in this study, specifically lower levels and earlier ages at the transition to declining cortisol output, which may represent an adaptive change in the HPA axis given the neurotoxic effects of prolonged cortisol exposure on neural structures (Carrion et al., 2007; McEwen et al., 2016).

There are several important limitations to this study that warrant consideration when evaluating the implications and generalizability of the results. First, the FGDS sample consists entirely of females sampled from a relatively low socioeconomic stratum. As such, these findings may not reflect cortisol changes over time for males exposed to CSA or those in higher socioeconomic stratums. Second, while this study measured multiple systems in the determination of biological embedding, epigenetic age acceleration was only assessed at one occasion when individuals were in their mid-30s, on average. While this approach identified those with the greatest change in resting cortisol secretion from childhood to adulthood following exposure to CSA, future research should investigate repeated assessments of epigenetic age acceleration that track concurrently or at some lag with repeated assessments of cortisol

concentrations in order to gain more insight into the dynamic interactions of these systems over time. Three, resting state cortisol was sampled predominantly in the morning hours, a time in the diurnal rhythm that appears most sensitive to detecting long-term change in the child maltreatment population (Bernard et al., 2017). Generalizations to trajectories of resting state cortisol secretion at other hours, such as afternoon or evening, are not warranted. Four, and related, the current study did not assess trajectories of cortisol stress reactivity measured in laboratory stressor paradigms or during the cortisol awakening response, dimensions of the HPA axis also related to child maltreatment (Holochwost et al., 2020). Finally, while the results provide evidence on the specific dimensions of resting state cortisol secretion change, it does not relate these changes to actual indicators of adulthood health. Thus, whether and how the biological embedding of CSA over the age range examined in this study predicts adverse adulthood health remains unknown.

5. Conclusions.

The major results from this analysis of 30-year longitudinal data are that accelerated epigenetic aging at mid-life was able to identify individuals with the most pronounced deviations in CSA-related HPA axis change, as evidenced by lower levels and earlier ages when peak cortisol concentrations are observed between six to forty-five years of age. These non-normative trends in HPA-axis functioning therefore serve as an indication of the biological embedding of early life adversity with potential implications for later adulthood health. Specifically, attenuation in cortisol profiles have been linked to a host of physical and behavioral health outcomes in adulthood following child maltreatment, including obesity (Li et al., 2021) and several different psychiatric disorders (Bremner et al., 2007; Kellner et al., 2018; Simsek et al., 2015). The risks for cortisol disruption, and therefore subsequent adulthood health, may be even greater for those with advanced epigenetic ages at mid-life. It will be important for future research to link child maltreatment, cortisol secretion changes, and epigenetic age acceleration to actual adulthood health outcomes in order to fully understand the implications of such biological embedding of early life adversity.

This study also advances a more specific and complete understanding of the biological embedding of early life adversity, namely the changes that occur in the HPA axis over repeated and extended periods of assessment, and points to aging biomarkers that predict several dimensions of HPA-axis change. Identifying aging biomarkers at mid-life has the potential to inform interventions during a time in life where many of the stress-related physical and behavioral health outcomes associated with aging have or will occur, providing needed information for targeted prevention of later-life outcomes. Future research should examine the relation between the biological embedding of early life adversity, including specific dimensions of HPA axis function, and various indicators of physical and behavioral health in adulthood to further establish such risks and guide targeted prevention.

References

Adam, E. K., Quinn, M. E., Tavernier, R., McQuillan, M. T., Dahlke, K. A., & Gilbert, K. E. (2017). Diurnal cortisol slopes and mental and physical health outcomes: A systematic review and meta-analysis. *Psychoneuroendocrinology, 83*, 25-41. https://doi.org/10.1016/j.psyneuen.2017.05.018

Alisic, E., Zalta, A. K., van Wesel, F., Larsen, S. E., Hafstad, G. S., Hassanpour, K., & Smid, G. E. (2014). Rates of post-traumatic stress disorder in trauma-exposed children and adolescents: Meta-analysis. *The British Journal of Psychiatry, 204*(5), 335-340. https://doi.org/http://dx.doi.org/10.1192/bjp.bp.113.131227

Anacker, C., O'Donnell, K. J., & Meaney, M. J. (2014). Early life adversity and the epigenetic programming of hypothalamic-pituitary-adrenal function. *Dialogues Clin Neurosci, 16*(3), 321-333.

Bernard, K., Frost, A., Bennett, C. B., & Lindhiem, O. (2017). Maltreatment and diurnal cortisol regulation: A meta-analysis. *Psychoneuroendocrinology, 78*, 57-67. https://doi.org/10.1016/j.psyneuen.2017.01.005

Bober, J. F., Weller, E. B., Weller, R. A., Tait, A., Fristad, M. A., & Preskorn, S. H. (1988). Correlation of serum and salivary cortisol levels in prepubertal school-aged children. *J Am Acad Child Adolesc Psychiatry, 27*(6), 748-750.

Bremner, D., Vermetten, E., & Kelley, M. E. (2007). Cortisol, dehydroepiandrosterone, and estradiol measured over 24 hours in women with childhood sexual abuse-related posttraumatic stress disorder. *J Nerv Ment Dis, 195*(11), 919-927. https://doi.org/10.1097/NMD.0b013e3181594ca0

Bürkner, P. C. (2017). brms: An R package for Bayesian multilevel models using Stan. *Journal of Statistical Software, 80*(1), 1-28.

Carrion, V. G., Weems, C. F., & Reiss, A. L. (2007). Stress predicts brain changes in children: A pilot longitudinal study on youth stress, posttraumatic stress disorder, and the hippocampus. *Pediatrics, 119*(3), 509-516.

http://search.ebscohost.com/login.aspx?direct=true&db=pbh&AN=24569686&loginpage=Login.asp&site=ehost-live&scope=site

Chang, C. C., Chow, C. C., Tellier, L. C., Vattikuti, S., Purcell, S. M., & Lee, J. J. (2015). Second-generation PLINK: rising to the challenge of larger and richer datasets. *Gigascience, 4*, 7. https://doi.org/10.1186/s13742-015-0047-8

Chen, B. H., Marioni, R. E., Colicino, E., Peters, M. J., Ward-Caviness, C. K., Tsai, P. C., Roetker, N. S., Just, A. C., Demerath, E. W., Guan, W., Bressler, J., Fornage, M., Studenski, S., Vandiver, A. R., Moore, A. Z., Tanaka, T., Kiel, D. P., Liang, L., Vokonas, P., Schwartz, J., Lunetta, K. L., Murabito, J. M., Bandinelli, S., Hernandez, D. G., Melzer, D., Nalls, M., Pilling, L. C., Price, T. R., Singleton, A. B., Gieger, C., Holle, R., Kretschmer, A., Kronenberg, F., Kunze, S., Linseisen, J., Meisinger, C., Rathmann, W., Waldenberger, M., Visscher, P. M., Shah, S., Wray, N. R., McRae, A. F., Franco, O. H., Hofman, A., Uitterlinden, A. G., Absher, D., Assimes, T., Levine, M. E., Lu, A. T., Tsao, P. S., Hou, L., Manson, J. E., Carty, C. L., LaCroix, A. Z., Reiner, A. P., Spector, T. D., Feinberg, A. P., Levy, D., Baccarelli, A., van Meurs, J., Bell, J. T., Peters, A., Deary, I. J., Pankow, J. S., Ferrucci, L., & Horvath, S. (2016). DNA methylation-based measures of biological age: meta-analysis predicting time to death. *Aging (Albany NY), 8*(9), 1844-1865. https://doi.org/10.18632/aging.101020

Dahmen, B., Puetz, V. B., Scharke, W., von Polier, G. G., Herpertz-Dahlmann, B., & Konrad, K. (2018). Effects of Early-Life Adversity on Hippocampal Structures and Associated HPA Axis Functions. *Dev Neurosci, 40*(1), 13-22. https://doi.org/10.1159/000484238

Davis, E. G., Humphreys, K. L., McEwen, L. M., Sacchet, M. D., Camacho, M. C., MacIsaac, J. L., Lin, D. T. S., Kobor, M. S., & Gotlib, I. H. (2017). Accelerated DNA methylation age in adolescent girls: associations with elevated diurnal cortisol and reduced hippocampal volume. *Transl Psychiatry, 7*(8), e1223. https://doi.org/10.1038/tp.2017.188

Del Giudice, M., Ellis, B. J., & Shirtcliff, E. A. (2011). The Adaptive Calibration Model of stress responsivity. *Neurosci Biobehav Rev, 35*(7), 1562-1592. https://doi.org/10.1016/j.neubiorev.2010.11.007

Fries, E., Hesse, J., Hellhammer, J., & Hellhammer, D. H. (2005). A new view on hypocortisolism. *Psychoneuroendocrinology, 30*(10), 1010-1016.

Gassen, N. C., Chrousos, G. P., Binder, E. B., & Zannas, A. S. (2017). Life stress, glucocorticoid signaling, and the aging epigenome: Implications for aging-related diseases. *Neurosci Biobehav Rev, 74*(Pt B), 356-365. https://doi.org/10.1016/j.neubiorev.2016.06.003

Gilbert, R., Widom, C. S., Browne, K., Fergusson, D., Webb, E., & Janson, S. (2009). Burden and consequences of child maltreatment in high-income countries. *Lancet, 373*(9657), 68-81. https://doi.org/10.1016/s0140-6736(08)61706-7

Goodyer, I. M., Herbert, J., Altham, P. M., Pearson, J., Secher, S. M., & Shiers, H. M. (1996). Adrenal secretion during major depression in 8- to 16-year-olds, I. Altered diurnal rhythms in salivary cortisol and dehydroepiandrosterone (DHEA) at presentation. *Psychol Med, 26*(2), 245-256.

Grimm, K. J., Ram, N., & Estabrook, R. (2017). *Growth Modeling: Structural Equation and Multi-level Modeling Approaches*. Guilford.

Handa, R. J., & Weiser, M. J. (2014). Gonadal steroid hormones and the hypothalamo-pituitary-adrenal axis. *Front Neuroendocrinol, 35*(2), 197-220. https://doi.org/10.1016/j.yfrne.2013.11.001

Hannum, G., Guinney, J., Zhao, L., Zhang, L., Hughes, G., Sadda, S., Klotzle, B., Bibikova, M., Fan, J. B., Gao, Y., Deconde, R., Chen, M., Rajapakse, I., Friend, S., Ideker, T., & Zhang, K. (2013). Genome-wide methylation profiles reveal quantitative views of human aging rates. *Mol Cell, 49*(2), 359-367. https://doi.org/10.1016/j.molcel.2012.10.016

Holochwost, S. J., Wang, G., Kolacz, J., Mills-Koonce, W. R., Klika, J. B., & Jaffee, S. R. (2020). The neurophysiological embedding of child maltreatment. *Dev Psychopathol*. https://doi.org/http://dx.doi.org/10.1017/S0954579420000383

Horvath, S. (2013). DNA methylation age of human tissues and cell types. *Genome Biol, 14*(10), R115. https://doi.org/10.1186/gb-2013-14-10-r115

Houseman, E. A., Accomando, W. P., Koestler, D. C., Christensen, B. C., Marsit, C. J., Nelson, H. H., Wiencke, J. K., & Kelsey, K. T. (2012). DNA methylation arrays as surrogate measures of cell mixture distribution. *BMC Bioinformatics, 13*, 86. https://doi.org/10.1186/1471-2105-13-86

Hughes, K., Bellis, M. A., Hardcastle, K. A., Sethi, D., Butchart, A., Mikton, C., Jones, L., & Dunne, M. P. (2017). The effect of multiple adverse childhood experiences on health: a systematic review and meta-analysis. *Lancet Public Health, 2*(8), e356-e366. https://doi.org/10.1016/s2468-2667(17)30118-4

Kaess, M., Whittle, S., O'Brien-Simpson, L., Allen, N. B., & Simmons, J. G. (2018). Childhood maltreatment, pituitary volume and adolescent hypothalamic-pituitary-adrenal axis—Evidence for a maltreatment-related attenuation. *Psychoneuroendocrinology, 98*, 39-45. https://doi.org/http://dx.doi.org/10.1016/j.psyneuen.2018.08.004

Kellner, M., Muhtz, C., Weinås, Å., Ćurić, S., Yassouridis, A., & Wiedemann, K. (2018). Impact of physical or sexual childhood abuse on plasma DHEA, DHEA-S and cortisol in a low-dose dexamethasone suppression test and on cardiovascular risk parameters in adult patients with major depression or anxiety disorders. *Psychiatry Res, 270*, 744-748. https://doi.org/10.1016/j.psychres.2018.10.068

Kruschke, J. K. (2015). Goals, Power, and Sample Size. In J. K. Kruschke (Ed.), *Doing Bayesian Data Analysis: A Tutorial with R, JAGS, and Stan* (Vol. 2nd Edition). Academic Press.

Kuzminskaite, E., Vinkers, C. H., Elzinga, B. M., Wardenaar, K. J., Giltay, E. J., & Penninx, B. (2020). Childhood trauma and dysregulation of multiple biological stress systems in adulthood: Results from the Netherlands Study of Depression and Anxiety (NESDA). *Psychoneuroendocrinology, 121*, 104835. https://doi.org/10.1016/j.psyneuen.2020.104835

Levine, M. E., Lu, A. T., Quach, A., Chen, B. H., Assimes, T. L., Bandinelli, S., Hou, L., Baccarelli, A. A., Stewart, J. D., Li, Y., Whitsel, E. A., Wilson, J. G., Reiner, A. P., Aviv, A., Lohman, K., Liu,

Y., Ferrucci, L., & Horvath, S. (2018). An epigenetic biomarker of aging for lifespan and healthspan. *Aging (Albany NY), 10*(4), 573-591. https://doi.org/10.18632/aging.101414

Li, J. C., Hall, M. A., Shalev, I., Schreier, H. M. C., Zarzar, T. G., Marcovici, I., Putnam, F. W., & Noll, J. G. (2021). Hypothalamic-pituitary-adrenal axis attenuation and obesity risk in sexually abused females. *Psychoneuroendocrinology, 129*, 105254. https://doi.org/10.1016/j.psyneuen.2021.105254

Lippard, E. T. C., & Nemeroff, C. B. (2020). The Devastating Clinical Consequences of Child Abuse and Neglect: Increased Disease Vulnerability and Poor Treatment Response in Mood Disorders. *Am J Psychiatry, 177*(1), 20-36. https://doi.org/10.1176/appi.ajp.2019.19010020

Lu, A. T., Quach, A., Wilson, J. G., Reiner, A. P., Aviv, A., Raj, K., Hou, L., Baccarelli, A. A., Li, Y., Stewart, J. D., Whitsel, E. A., Assimes, T. L., Ferrucci, L., & Horvath, S. (2019). DNA methylation GrimAge strongly predicts lifespan and healthspan. *Aging (Albany NY), 11*(2), 303-327. https://doi.org/10.18632/aging.101684

Lu, A. T., Xue, L., Salfati, E. L., Chen, B. H., Ferrucci, L., Levy, D., Joehanes, R., Murabito, J. M., Kiel, D. P., Tsai, P. C., Yet, I., Bell, J. T., Mangino, M., Tanaka, T., McRae, A. F., Marioni, R. E., Visscher, P. M., Wray, N. R., Deary, I. J., Levine, M. E., Quach, A., Assimes, T., Tsao, P. S., Absher, D., Stewart, J. D., Li, Y., Reiner, A. P., Hou, L., Baccarelli, A. A., Whitsel, E. A., Aviv, A., Cardona, A., Day, F. R., Wareham, N. J., Perry, J. R. B., Ong, K. K., Raj, K., Lunetta, K. L., & Horvath, S. (2018). GWAS of epigenetic aging rates in blood reveals a critical role for TERT. *Nat Commun, 9*(1), 387. https://doi.org/10.1038/s41467-017-02697-5

Marioni, R. E., Shah, S., McRae, A. F., Chen, B. H., Colicino, E., Harris, S. E., Gibson, J., Henders, A. K., Redmond, P., Cox, S. R., Pattie, A., Corley, J., Murphy, L., Martin, N. G., Montgomery, G. W., Feinberg, A. P., Fallin, M. D., Multhaup, M. L., Jaffe, A. E., Joehanes, R., Schwartz, J., Just, A. C., Lunetta, K. L., Murabito, J. M., Starr, J. M., Horvath, S., Baccarelli, A. A., Levy, D., Visscher, P. M., Wray, N. R., & Deary, I. J. (2015). DNA methylation age of blood predicts all-cause mortality in later life. *Genome Biology, 16*, 25. https://doi.org/10.1186/s13059-015-0584-6

McArdle, J. J., & Woodcock, R. W. (1997). Expanding test–retest designs to include developmental time-lag components. *Psychological Methods, 2*(4), 403-435. https://doi.org/http://dx.doi.org/10.1037/1082-989X.2.4.403

McCarthy, S., Das, S., Kretzschmar, W., Delaneau, O., Wood, A. R., Teumer, A., Kang, H. M., Fuchsberger, C., Danecek, P., Sharp, K., Luo, Y., Sidore, C., Kwong, A., Timpson, N., Koskinen, S., Vrieze, S., Scott, L. J., Zhang, H., Mahajan, A., Veldink, J., Peters, U., Pato, C., van Duijn, C. M., Gillies, C. E., Gandin, I., Mezzavilla, M., Gilly, A., Cocca, M., Traglia, M., Angius, A., Barrett, J. C., Boomsma, D., Branham, K., Breen, G., Brummett, C. M., Busonero, F., Campbell, H., Chan, A., Chen, S., Chew, E., Collins, F. S., Corbin, L. J., Smith, G. D., Dedoussis, G., Dorr, M., Farmaki, A. E., Ferrucci, L., Forer, L., Fraser, R. M., Gabriel, S., Levy, S., Groop, L., Harrison, T., Hattersley, A., Holmen, O. L., Hveem, K., Kretzler, M., Lee, J. C., McGue, M., Meitinger, T., Melzer, D., Min, J. L., Mohlke, K. L., Vincent, J. B., Nauck, M., Nickerson, D., Palotie, A., Pato, M., Pirastu, N., McInnis, M., Richards, J. B., Sala, C., Salomaa, V., Schlessinger, D., Schoenherr, S., Slagboom, P. E., Small, K., Spector, T., Stambolian, D., Tuke, M., Tuomilehto, J., Van den Berg, L. H., Van Rheenen, W., Volker, U., Wijmenga, C., Toniolo, D., Zeggini, E., Gasparini, P., Sampson, M. G., Wilson, J. F., Frayling, T., de Bakker, P. I., Swertz, M. A., McCarroll, S., Kooperberg, C., Dekker, A., Altshuler, D., Willer, C., Iacono, W., Ripatti, S., Soranzo, N., Walter, K., Swaroop, A., Cucca, F., Anderson, C. A., Myers, R. M., Boehnke, M., McCarthy, M. I., Durbin, R., & Haplotype Reference, C. (2016). A reference panel of 64,976 haplotypes for genotype imputation. *Nat Genet, 48*(10), 1279-1283. https://doi.org/10.1038/ng.3643

McEwen, B. S. (2007). Physiology and neurobiology of stress and adaptation: central role of the brain. *Physiol Rev, 87*(3), 873-904.

McEwen, B. S., Nasca, C., & Gray, J. D. (2016). Stress Effects on Neuronal Structure: Hippocampus, Amygdala, and Prefrontal Cortex. *Neuropsychopharmacology, 41*(1), 3-23. https://doi.org/10.1038/npp.2015.171

Miller, G. E., Chen, E., & Zhou, E. S. (2007). If it goes up, must it come down? Chronic stress and the hypothalamic-pituitary-adrenocortical axis in humans. *Psychological Bulletin, 133*(1), 25-45. https://doi.org/10.1037/0033-2909.133.1.25

Miller, R., Stalder, T., Jarczok, M., Almeida, D. M., Badrick, E., Bartels, M., Boomsma, D. I., Coe, C. L., Dekker, M. C., Donzella, B., Fischer, J. E., Gunnar, M. R., Kumari, M., Lederbogen, F., Power, C., Ryff, C. D., Subramanian, S. V., Tiemeier, H., Watamura, S. E., & Kirschbaum, C. (2016). The CIRCORT database: Reference ranges and seasonal changes in diurnal salivary cortisol derived from a meta-dataset comprised of 15 field studies. *Psychoneuroendocrinology, 73*, 16-23. https://doi.org/10.1016/j.psyneuen.2016.07.201

Noll, J. G., Trickett, P. K., Long, J. D., Negriff, S., Susman, E. J., Shalev, I., Li, J. C., & Putnam, F. W. (2017). Childhood Sexual Abuse and Early Timing of Puberty. *J Adolesc Health, 60*(1), 65-71. https://doi.org/10.1016/j.jadohealth.2016.09.008

O'Donnell, K. J., Glover, V., Jenkins, J., Browne, D., Ben-Shlomo, Y., Golding, J., & O'Connor, T. G. (2013). Prenatal maternal mood is associated with altered diurnal cortisol in adolescence. *Psychoneuroendocrinology, 38*(9), 1630-1638. https://doi.org/10.1016/j.psyneuen.2013.01.008

Oh, D. L., Jerman, P., Silverio Marques, S., Koita, K., Purewal Boparai, S. K., Burke Harris, N., & Bucci, M. (2018). Systematic review of pediatric health outcomes associated with childhood adversity. *BMC Pediatr, 18*(1), 83. https://doi.org/10.1186/s12887-018-1037-7

Pan, X., Wang, Z., Wu, X., Wen, S. W., & Liu, A. (2018). Salivary cortisol in post-traumatic stress disorder: a systematic review and meta-analysis. *BMC Psychiatry, 18*(1), 324. https://doi.org/10.1186/s12888-018-1910-9

Patterson, N., Price, A. L., & Reich, D. (2006). Population structure and eigenanalysis. *PLoS Genet, 2*(12), e190. https://doi.org/10.1371/journal.pgen.0020190

Raj, K., & Horvath, S. (2020). Current perspectives on the cellular and molecular features of epigenetic ageing. *Exp Biol Med (Maywood), 245*(17), 1532-1542. https://doi.org/10.1177/1535370220918329

Riis, J. L., Chen, F. R., Dent, A., Laurent, H. K., & Bryce, C. I. (2020). Analytical strategies and tactics in salivary bioscience. In D. A. Granger & M. K. Taylor (Eds.), *Salivary Bioscience: Foundations of Interdisciplinary Saliva Research and Applications* (pp. 49-87). Springer.

Rosmalen, J. G., Oldehinkel, A. J., Ormel, J., de Winter, A. F., Buitelaar, J. K., & Verhulst, F. C. (2005). Determinants of salivary cortisol levels in 10-12 year old children; a population-based study of individual differences. *Psychoneuroendocrinology, 30*(5), 483-495.

Schreiber, J. E., Shirtcliff, E., Van Hulle, C., Lemery-Chalfant, K., Klein, M. H., Kalin, N. H., Essex, M. J., & Goldsmith, H. H. (2006). Environmental influences on family similarity in afternoon cortisol levels: twin and parent-offspring designs. *Psychoneuroendocrinology, 31*(9), 1131-1137. https://doi.org/10.1016/j.psyneuen.2006.07.005

Shenk, C. E., Noll, J. G., Peugh, J. L., Griffin, A. M., & Bensman, H. E. (2016). Contamination in the prospective study of child maltreatment and female adolescent health. *Journal of Pediatric Psychology, 41*, 37-45. https://doi.org/10.1093/jpepsy/jsv017

Silverman, M. N., Pearce, B. D., Biron, C. A., & Miller, A. H. (2005). Immune modulation of the hypothalamic-pituitary-adrenal (HPA) axis during viral infection. *Viral Immunol, 18*(1), 41-78. https://doi.org/10.1089/vim.2005.18.41

Simmons, J. G., Byrne, M. L., Schwartz, O. S., Whittle, S. L., Sheeber, L., Kaess, M., Youssef, G. J., & Allen, N. B. (2015). Dual-axis hormonal covariation in adolescence and the moderating influence of prior trauma and aversive maternal parenting. *Dev Psychobiol, 57*(6), 670-687. https://doi.org/10.1002/dev.21275

Simsek, S., Uysal, C., Kaplan, I., Yuksel, T., & Aktas, H. (2015). BDNF and cortisol levels in children with or without post-traumatic stress disorder after sustaining sexual abuse. *Psychoneuroendocrinology, 56*, 45-51. https://doi.org/10.1016/j.psyneuen.2015.02.017

Törnhage, C. J. (2002). Reference values for morning salivary cortisol concentrations in healthy school-aged children. *J Pediatr Endocrinol Metab, 15*(2), 197-204. https://doi.org/10.1515/jpem.2002.15.2.197

Triche, T. J., Jr., Weisenberger, D. J., Van Den Berg, D., Laird, P. W., & Siegmund, K. D. (2013). Low-level processing of Illumina Infinium DNA Methylation BeadArrays. *Nucleic Acids Res, 41*(7), e90. https://doi.org/10.1093/nar/gkt090

Trickett, P. K., Noll, J. G., & Putnam, F. W. (2011). The impact of sexual abuse on female development: Lessons from a multigenerational, longitudinal research study. *Dev Psychopathol, 23*, 453-476. https://doi.org/10.1017/S095457941000174

Trickett, P. K., Noll, J. G., Susman, E. J., Shenk, C. E., & Putnam, F. W. (2010). Attenuation of cortisol across development for victims of sexual abuse. *Dev Psychopathol, 22*(1), 165-175. https://doi.org/10.1017/s0954579409990332

[Record #625 is using a reference type undefined in this output style.]

Ulrich-Lai, Y. M., & Ryan, K. K. (2014). Neuroendocrine circuits governing energy balance and stress regulation: functional overlap and therapeutic implications. *Cell Metab, 19*(6), 910-925. https://doi.org/10.1016/j.cmet.2014.01.020

Young, E. A. (1995). The role of gonadal steroids in hypothalamic-pituitary-adrenal axis regulation. *Crit Rev Neurobiol, 9*(4), 371-381.

Zannas, A. S. (2019). Epigenetics as a key link between psychosocial stress and aging: concepts, evidence, mechanisms. *Dialogues Clin Neurosci, 21*(4), 389-396. https://doi.org/10.31887/DCNS.2019.21.4/azannas

Zannas, A. S., Arloth, J., Carrillo-Roa, T., Iurato, S., Roh, S., Ressler, K. J., Nemeroff, C. B., Smith, A. K., Bradley, B., Heim, C., Menke, A., Lange, J. F., Bruckl, T., Ising, M., Wray, N. R., Erhardt, A., Binder, E. B., & Mehta, D. (2015). Lifetime stress accelerates epigenetic aging in an urban, African American cohort: relevance of glucocorticoid signaling. *Genome Biol, 16*, 266. https://doi.org/10.1186/s13059-015-0828-5

Table 1.

Results for Child Sexual Abuse and Epigenetic Age Acceleration in the Horvath and Hannum Clocks

Fixed Effects		Horvath				Hannum			
Main Effects	Interaction Effects	Est.	se	CI	PD	Est.	se	CI	PD
Intercept, γ_{00}		12.31	0.57	11.15, 13.39	**100.00**	12.41	0.53	11.37, 13.45	**100.00**
	Group, γ_{01}	-0.84	0.83	-2.45, 0.80	**84.80**	-1.43	0.95	-3.26. 0.41	**93.27**
	EpiAge, γ_{02}	0.19	0.18	-0.19, 0.51	**87.67**	0.09	0.18	-0.26, 0.44	69.27
	GroupXEpiAge, γ_{03}	-0.39	0.26	-0.89 0.15	**93.13**	-0.49	0.34	-1.15, 0.18	**92.68**
Slope 1, γ_{10}		0.25	0.06	0.13, 0.37	**99.99**	0.27	0.05	0.16, 0.38	**100.00**
	Group, γ_{11}	0.12	0.18	-0.18, 0.52	74.83	0.22	0.26	-0.19, 0.83	**80.23**
	EpiAge, γ_{12}	-0.02	0.02	-0.07, 0.02	**83.59**	0.01	0.02	-0.03, 0.05	**75.00**
	GroupXEpiAge, γ_{13}	0.04	0.04	-0.03, 0.12	**88.80**	0.08	0.13	-0.10, 0.36	64.82
Slope 2, γ_{20}		-0.36	0.06	-0.47, -0.24	**100.00**	-0.37	0.06	-0.48, -0.26	**100.00**
	Group, γ_{21}	-0.10	0.17	-0.49, 0.19	71.98	-0.18	0.24	-0.75, 0.19	**76.33**
	EpiAge, γ_{22}	0.00	0.02	-0.04, 0.05	54.90	-0.02	0.02	-0.06, 0.02	**82.38**
	GroupXEpiAge, γ_{23}	-0.01	0.04	-0.10, 0.06	61.08	-0.04	0.13	-0.32, 0.16	53.46
Knot, γ_{30}		4.65	1.59	1.78, 8.05	**99.64**	4.27	1.19	2.07, 6.73	**99.95**
	Group, γ_{31}	-3.06	2.55	-7.64, 2.72	**89.60**	-3.58	2.67	-7.82, 3.10	**90.06**

	EpiAge, γ_{32}	0.49	0.55	-0.51, 1.52	**86.07**	-0.29	0.46	-1.15, 0.67	**75.76**
	GroupXEpiAge, γ_{33}	-0.77	0.68	-2.06, 0.64	**89.66**	-0.65	1.35	-3.11, 1.93	66.22
PC1, γ_{04}		1.30	3.89	-6.26, 8.94	63.16	2.19	3.68	-5.15, 9.41	72.83
PC2, γ_{05}		-0.50	3.57	-7.51, 6.54	55.85	-1.04	3.39	-7.67, 5.67	62.40
PC3, γ_{06}		-2.23	3.65	-9.28, 5.12	73.86	-1.85	3.53	-8.59, 5.46	71.43
Random Effects									
SDs	Correlations	Est.	se	CI		Est.	se	CI	
Intercept, σ_{u0}		0.99	0.58	0.06, 2.28	-	1.07	0.58	0.08, 2.37	-
	Slope 1, r_{u0u1}	-0.06	0.46	-0.86, 0.80	-	0.08	0.45	-0.78, 0.84	-
	Slope 2, r_{u0u2}	-0.22	0.45	-0.90, 0.72	-	-0.25	0.46	-0.91, 0.72	-
	Knot, r_{u0u3}	0.23	0.45	-0.72, 0.90	-	0.28	0.44	-0.69, 0.91	-
Slope 1, σ_{u1}		0.05	0.04	0.00, 0.14	-	0.05	0.03	0.00, 0.13	-
	Slope 2, r_{u1u2}	-0.09	0.45	-0.85, 0.78	-	-0.09	0.45	-0.85, 0.78	-
	Knot, r_{u1u3}	-0.22	0.46	-0.92, 0.72	-	-0.12	0.45	-0.86, 0.76	-
Slope 2, σ_{u2}		0.06	0.05	0.00, 0.17	-	0.06	0.05	0.00, 0.18	-
	Knot, r_{u2u3}	0.10	0.45	-0.77, 0.86	-	-0.02	0.45	-0.82, 0.81	-
Knot, σ_{u3}		1.87	1.03	0.14, 4.20	-	1.33	0.80	0.07, 3.01	-
Sigma, σ_{e}		3.34	0.16	3.03, 3.65	-	3.34	0.16	3.04, 3.65	-

Note: N = 402 observations nested within 86 persons. Bold indicates a probability of direction above 75% and a potentially meaningful effect. Intercept is the level of cortisol at the knot location; Slope 1 is the rate of change in cortisol during the early (pre-knot) phase; Slope 2 is the rate of change in cortisol during the later (post-knot) phase; Knot is the age at which cortisol trajectories change from the early to the late phase (estimate is the number of years added to the centered age variable); PC1-PC3 are principal component estimates to control for population stratification of ethnicity; Est. is the fixed effects population estimate; se is the standard error of that estimate; CI is the Bayesian 95% credibility interval; PD = probability of the direction (positive or negative) of the observed effect

Table 2.

Results for Child Sexual Abuse and Epigenetic Age Acceleration in the GrimAge and PhenoAge Clocks

Fixed Effects		GrimAge				PhenoAge			
Main Effects	Interaction Effects	Est.	se	CI	PD	Est.	se	CI	PD
Intercept, γ_{00}		11.26	1.19	8.98, 13.64	**100.00**	10.88	1.18	8.74, 13.32	**100.00**
	Group, γ_{01}	-1.11	1.02	-3.37, 0.68	**88.69**	-1.16	1.01	-3.38, 0.59	**89.69**
	EpiAge, γ_{02}	0.01	0.09	-0.19, 0.19	55.33	-0.08	0.09	-0.27, 0.08	**83.68**
	GroupXEpiAge, γ_{03}	-0.09	0.18	-0.45, 0.28	70.66	-0.07	0.15	-0.36, 0.25	69.01
Slope 1, γ_{10}		0.25	0.06	0.14, 0.36	**100.00**	0.25	0.06	0.14, 0.36	**100.00**
	Group, γ_{11}	0.10	0.17	-0.19, 0.49	71.01	0.09	0.16	-0.18, 0.41	71.12
	EpiAge, γ_{12}	-0.01	0.01	-0.03, 0.01	**76.49**	0.00	0.01	-0.02, 0.02	68.55
	GroupXEpiAge, γ_{13}	0.01	0.03	-0.04, 0.07	67.99	0.02	0.02	-0.02, 0.05	**84.72**
Slope 2, γ_{20}		-0.35	0.06	-0.47, -0.24	**100.00**	-0.36	0.06	-0.48, -0.25	**100.00**
	Group, γ_{21}	-0.11	0.17	-0.49, 0.18	74.11	-0.08	0.15	-0.09, 018	70.64
	EpiAge, γ_{22}	0.00	0.01	-0.02, 0.03	53.93	0.00	0.01	-0.01, 0.02	69.29
	GroupXEpiAge, γ_{23}	-0.01	0.03	-0.07, 0.04	67.89	-0.02	0.02	-0.06, 0.01	**87.87**
Knot, γ_{30}		4.40	1.34	1.99, 7.26	**99.88**	4.61	1.33	2.16, 7.35	**99.88**
	Group, γ_{31}	-2.93	2.32	-7.25, 1.98	**91.23**	-2.19	2.22	-6.22, 2.49	**85.50**

	EpiAge, γ_{32}	0.08	0.21	-0.34, 0.52	66.26	0.06	0.23	-0.46, 0.46	64.64
	GroupXEpiAge, γ_{33}	-0.40	0.39	-1.18, 0.38	**86.62**	-0.37	0.32	-0.96, 0.34	**88.51**
PC1, γ_{04}		0.14	3.91	-7.47, 7.92	51.08	0.16	3.82	-7.29, 7.70	51.64
PC2, γ_{05}		-1.24	3.65	-8.38, 6.01	63.67	-1.49	3.33	-8.02, 5.13	67.69
PC3, γ_{06}		-1.44	3.78	-8.87, 6.10	65.25	0.04	3.83	-7.46, 7.61	50.22
Gran, γ_{07}		-4.43	4.22	-12.53, 3.90	**86.62**	-6.98	4.35	-14.87, 1.80	**93.98**
CD4T, γ_{08}		-2.07	4.31	-10.45, 6.48	68.66	-0.17	4.42	-8.70, 8.55	51.95
CD8T, γ_{09}		0.89	4.70	-8.33, 10.10	57.60	0.24	4.68	-8.93, 9.42	52.26
NK, γ_{010}		0.29	4.89	-9.29, 9.89	52.42	-0.09	4.9	-9.62, 9.51	50.61
Mono, γ_{011}		1.61	4.89	-8.04, 11.12	63.07	1.24	4.84	-8.24, 10.65	60.15
Random Effects									
SDs	Correlations	Est.	se	CI		Est.	se	CI	
Intercept, σ_{u0}		0.98	0.52	0.08, 2.07	-	0.81	0.49	0.05, 1.88	-
	Slope 1, r_{u0u1}	0.08	0.45	-0.79, 0.85	-	0.13	0.44	-0.75, 0.86	-
	Slope 2, r_{u0u2}	-0.27	0.44	-0.90, 0.68	-	-0.30	0.44	-0.92, 0.66	-
	Knot, r_{u0u3}	0.16	0.44	-0.73, 0.87	-	0.14	0.44	-0.75, 0.86	-
Slope 1, σ_{u1}		0.05	0.04	0.00, 0.15	-	0.06	0.04	0.00, 0.15	-
	Slope 2, r_{u1u2}	-0.13	0.45	-0.87, 0.76	-	-0.23	0.45	-0.91, 0.71	-

	Knot, r_{u1u3}	-0.20	0.45	-0.90, 0.73	-	-0.17	0.45	-0.89, 0.75	-
Slope 2, σ_{u2}		0.09	0.06	0.00, 0.23	-	0.12	0.08	0.01, 0.28	-
	Knot, r_{u2u3}	0.00	0.45	-0.81, 0.80	-	-0.03	0.45	-0.82, 0.80	-
Knot, σ_{u3}		1.42	0.88	0.08, 3.35	-	1.24	0.78	0.06, 2.91	-
Sigma, σ_e		3.33	0.16	3.02, 3.65	-	3.31	0.16	2.99, 3.63	-

Note: N = 402 observations nested within 86 persons. Bold indicates a probability of direction above 75% and a potentially meaningful effect. Intercept is the level of cortisol at the knot location; Slope 1 is the rate of change in cortisol during the early (pre-knot) phase; Slope 2 is the rate of change in cortisol during the later (post-knot) phase; Knot is the age at which cortisol trajectories change from the early to the late phase (estimate is the number of years added to the centered age variable); PC1-PC3 are principal component estimates to control for population stratification of ethnicity; Gran, CD4T, CD8T, NK, and Mono are control variables for different cell counts; Est. is the fixed effects population estimate; se is the standard error of that estimate; CI is the Bayesian 95% credibility interval; PD = probability of the direction (positive or negative) of the observed effect.

Figure 1.

Observed Individual Trajectories (gray) and Prototypical Trajectory (black) of Cortisol Concentrations Across Childhood, Adolescence, and Adulthood.

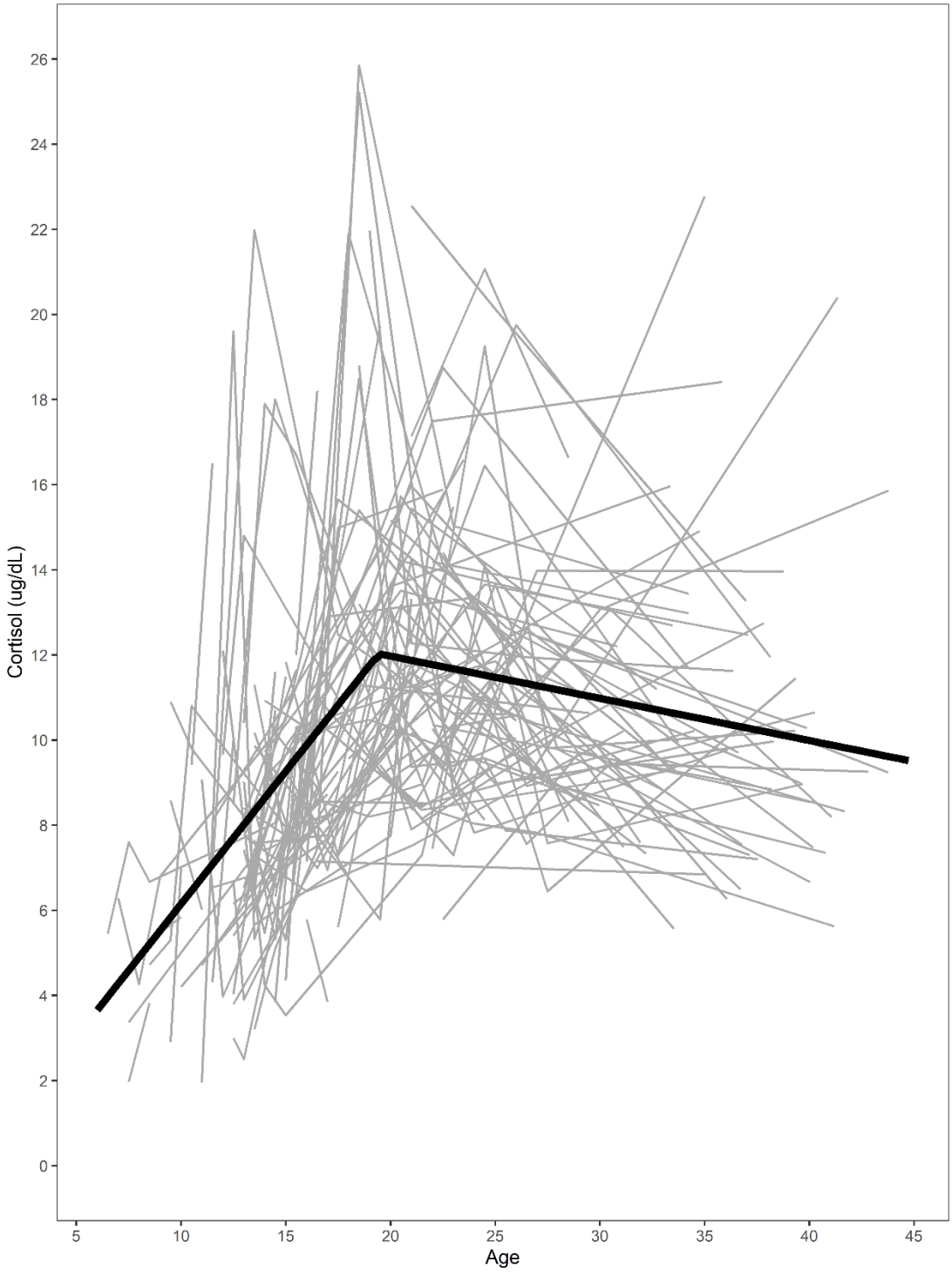

Figure 2.

Relations among Childhood Sexual Abuse, Epigenetic Age Acceleration via the Horvath and Hannum Clocks, and Cortisol Growth as Obtained from Conditional Bilinear Spline Growth Model

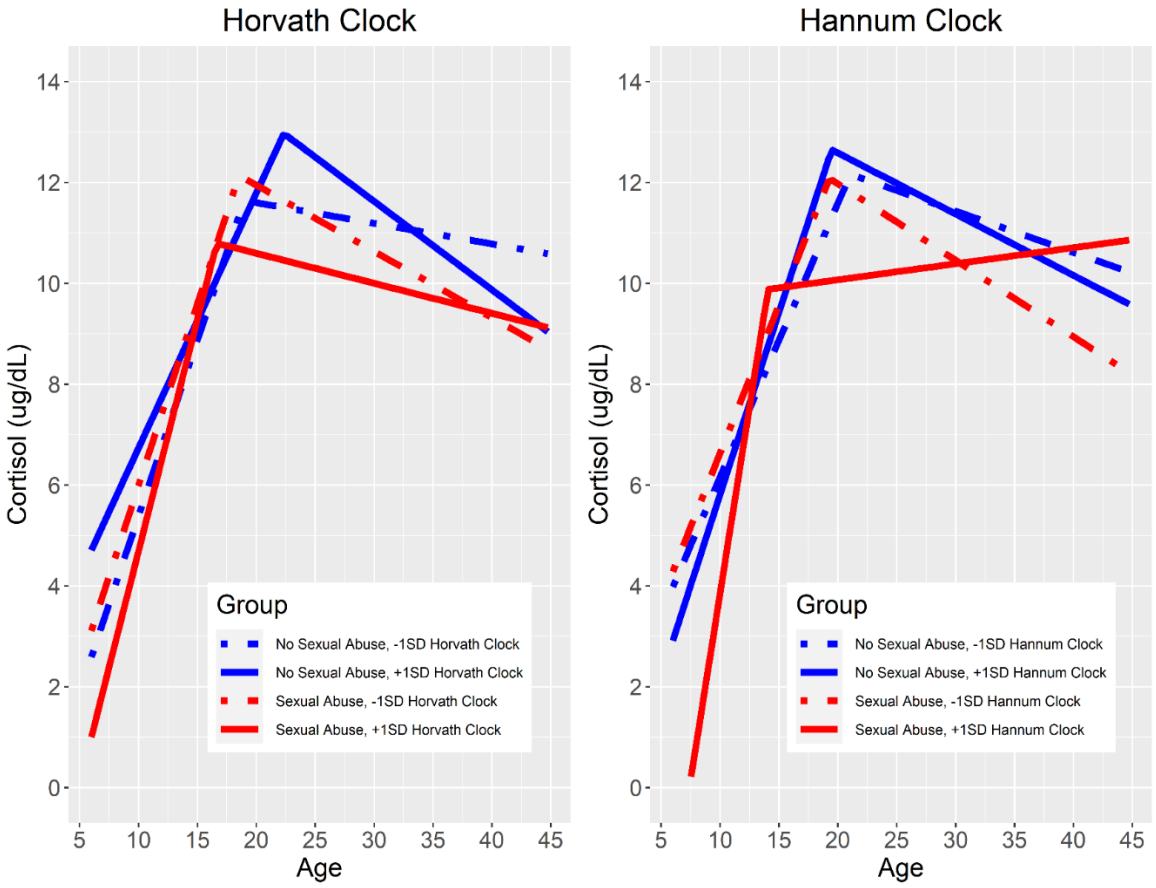

Figure 3.

Relations among Childhood Sexual Abuse, Epigenetic Age Acceleration via the PhenoAge and GrimAge Clocks, and Cortisol Growth as Obtained from Conditional Bilinear Spline Growth Model